Selective detection of organophosphate through molecularly imprinted GERS-active hybrid organic–inorganic materials

Selective detection of organophosphate through molecularly imprinted GERS-active hybrid organic–inorganic materials

D. Carboni,[a†] Y. Jiang,[a†] L. Malfatti[a,b] and P. Innocenzi[a*]

** Correspondence to: P. Innocenzi, Laboratorio di Scienza dei Materiali e Nanotecnologie, Dipartimento di Chimica e Farmacia, Università di Sassari, CR-INSTM, Via Vienna, 2, Sassari 07100, Italy.*
E-mail: plinio@uniss.it

† D. Carboni and Y. Jiang contributed equally to this work

a Laboratorio di Scienza dei Materiali e Nanotecnologie, Dipartimento di Chimica eFarmacia, Università di Sassari, CR-INSTM, Via Vienna, 2, Sassari 07100, Italy

b Istituto dei Polimeri, Compositi e Biomateriali- IPCB – CNR, Via Campi Flegrei, 34, Pozzuoli 80078, NA, Italy

A selective sensing platform for the organophosphate paraoxon, a highly toxic organic pollutant, has been designed and tested on water samples. A porous hybrid organic–inorganic film, synthesised using tetraethoxysilane, 1,8-bis(triethoxysilyl) octane and cetyltrimethylammonium bromide, has been molecularly imprinted with a structural analogue of paraoxon, the diethyl(4-nitrobenzyl)phosphonate, to induce selective recognition. Exfoliated graphene has been incorporated into the porous matrix to provide enhancement of the Raman scattering signal. The Raman sensor has been tested on different concentrations of paraoxon in both ethanol and water/ethanol mixture. The molecular selectivity has been assessed by comparing the Raman signal enhancement of paraoxon with a similar organophosphate, the bis-(4-nitrophenyl) phosphate. The molecularly imprinted film has shown a fourfold increase of the paraoxon signal, when compared with the corresponding not-imprinted. The evaluation of the density of molecular cavities into the molecularly imprinted samples ($4.50 * 10^{-10}$ μmol $μm^{-3}$) has allowed assuming that each molecular cavity is capable of providing a remarkable signal enhancement of $1.47 * 10^{12}$ count * $μmol^{-1}$ only when recognising paraoxon. The material design has allowed coupling the sensitivity of the graphene-mediated enhancement of Raman scattering with the selectivity of molecular imprinting into a single and potentially portable, analytical system.

Keywords: organophosphates; GERS; molecular imprinting; hybrid materials; pesticides

Introduction

The detection of a specific analyte in complex mixtures, especially in water samples or biological fluids, requires operating a sequence involving a separation procedure followed by detection. Hyphen- ated techniques such as liquid chromatography coupled with mass spectrometry or with nuclear magnetic resonance are commonly employed. However, these methods, although very selective and accurate, involve two potentially time-consuming sequential steps operated by different techniques. For this reason, the most recent developments of analytical devices point out towards the use of advanced functional materials capable of performing two operational steps, identification and quantification, into a single device.[1,2] These approaches are very important in monitoring persisting highly toxic organic pollutants in complex environmental matrices such as ground water or soil. Organophosphates (OPs) are one of the most widespread classes of pollutants among the highly toxic organic pollutants, and they are closely related to lethal chemical warfare agents such as sarin.[3] The persistency in the environment represents a high threat for the human health because it can span from few months up to several years depend- ing on their half-lives and upon the medium they are dispersed in.[4] The high toxicity of the OPs is related to their capability of inhibiting irreversibly the mammalian acetyl-cholinesterase. This neurotoxic effect can produce serious damages to the central nervous system causing neurodevelopmental deficits in young children[5,6] and also death. For this reason, the need for environmental monitoring of these species has raised a growing demand for

systems capableof inactivating them.[7–9] Alternatively, fast and reliable sensing devices able of quantitative monitoring their concentration inwater samples are highly sought after.[10] In recent years, the increasing request of sensing devices for OPs compound has seen a plethora of new approaches being explored by different research groups.[11] An interesting overview of recent advancements in the techniques used for organophosphate detection and corresponding detection limits has been recently reported by Kumar et al.[12] The biosensors mainly based on enzymatic inhibition of acetyl-cholinesterase[13] or immnunochemistry[14] seem to be the most efficient in term of sensitivity (because they can reach detection limits of 0.1 pM for paraoxon detection). However, most of these sensors present some drawbacks that are peculiar of protein-based systems, such as long measuring times and limitations because of pH, temperature and solvents. Important achievements have been recently reached by using advanced functional materials making use of carbon nanotubes,[15] graphene,

metal–organic frameworks,[16] molecularly imprinted materials[17] and both inorganic[18] and organic[19] quantum dots. Molecularly imprinted materials, in particular, have proved to be easy to handle, cost-effective, portable, and with good sensitivity, reliability and reproducibility.[20] Moreover, they are characterised by an excellent molecular selectivity that makes them an exceptional separationtechnique.

One of the most sensitive techniques for pesticide detection makes use of the surface enhanced Raman scattering provided by metal plasmon surfaces (Ag, Au nanoparticles).[21] However, these approaches have the disadvantage of using mostly noble metals, and they must be often coupled with a separation technique to avoid the interferences due to complex matrices and structural analogues. However, a new enhancement of Raman scattering (ERS) effect mediated by graphene (GERS),[22] or graphene in dielectric systems for non-plasmonic SERS applications,[23] which allows avoiding the use of noble metals, has been recently discovered.[24] This effect is mostly due to chemical enhancement rather than electromagnetic, such as in the case of metallic particles. The interaction through the π π bonding of aromatic molecules with thesmooth surface of graphene promotes charge transfer and therefore chemical enhancement.

Our laboratory has developed different approaches to investigate this effect by incorporating exfoliated graphene into porous films[25,26] and by exploiting a considerable experience in synthesising hybrid films.[27]

In particular, to overcome the drawbacks of the common hyphenated approaches, we have recently developed a sensing system that is able of coupling a separation technique for selective solid phase extraction, the molecular imprinting (MI), with a sensitive and cost-effective detection technique, the GERS.[28] The pairing of these two techniques, which we have named MI-GERS, Molecularly Imprinted - Graphene-mediated Enhancement of Raman Scattering, can be considered as a new kind of hyphenated approach capable of performing a selective recognition and a quantitative detection of a specific analyte into a single platform. In a previous work, we have successfully developed and tested a GERS platform using Rhodamine 6G as a sensing probe. We have now extended the GERS sensing system to test a real pollutant molecule in an aqueous environment, and we have therefore designed again the material to be used in water and reused several times.

The present work aims at developing the first application of the MI-GERS active substrates by targeting the detection of a highlytoxic organophosphate pesticide, paraoxon, using a specifically designed MI-GERS hybrid platform.

Results and discussion

Material design of the sensing platform

A hybrid organic–inorganic material has been chosen to design a graphene-based sensor because this offered the great advantage of tailoring the matrix according to the chemical structure of the target analyte. In fact, the high flexibility of the hybrid matrix and the sol–gel process allowed preparing porous nanocomposites with molecularly imprinted cavities. However, to maximise the affinity between analyte and matrix, a careful tuning of the hydrophobicity is required. The hybrid organic–inorganic matrix has been, therefore, designed by following this rational and the specific requirements dictated by the environmental target, the diethyl- 4-nitrophenyl phosphate, marketed as paraoxon (Figure 1). The MI strategy is based on the synthesis of a solid-state matrix around a chosen molecular structure that acts as a template for imprinting 3D cavities. After its removal, the molecular cavities are able to recognise the template or very close structural

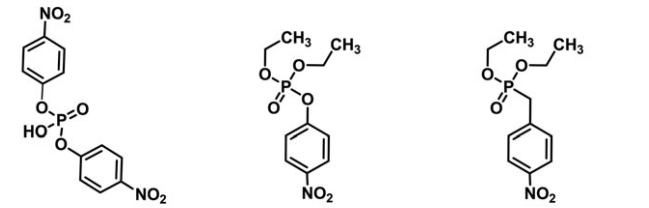

Figure 1. Molecular structures of diethyl(4-nitrobenzyl)phosphonate (4NBP), paraoxon and bis(4-nitrophenyl) phosphate (B4NPP).

analogues (Figure 2). Our group has already demonstrated that the presence of graphene embedded into porous matrices is capable of enhancing the Raman signal of adsorbed molecules.[25] In the present system, however, the molecular cavities must recognise a specific analyte and then promote a selective enhancement of its Raman signal exploiting the amplification mediated by the graphene embedded into the porous material. This makes the synthesis of the hybrid matrix particularly challenging and a new design of the sensing platform, which has to fulfil specific requirements has been realised. The resulting matrix, in fact, should be stiff enough to ensure both mechanical and hydrolytic stabilities in water/ethanol mixtures and flexible enough to allow removal of the molecular template and selective rebinding of paraoxon. We have used various combinations of different hybrid precursors (tetraethoxysilane, methyltriethoxysilane, 3- trimethoxysilylpropyl-methacrylate, vinyltriethoxysilane, phenyl- triethoxysilane and diphenyldiethoxysilane), however none of these combinations resulted suitable for the imprinting procedure. In some cases, it was difficult to remove the molecular template from the matrix, and in other samples, the matrix could not withstand the washing procedure needed to repeat the measurements. Moreover, the use of highly hydrophobic precursors made too difficult to deposit the water droplets containing pesticides. Among the pool of precursors, the combination tetraethoxysilane-1,8-bis(triethoxysilyl)octane ensured the best compromise between MI procedure, matrix stability (both thermal and hydrolytic) and surface hydrophilicity. The optimised hybrid material have been therefore synthesised by using a 1:1 ratio of tetraethoxysilane and 1,8-bis(triethoxysilyl)octane.

The Raman spectra of exfoliated graphene (EG) upon dispersion in *N*-Vinyl-2-pyrrolidone (NVP) (bottom curve) and incorporation in NIF (Not Imprinted Films) samples (top curve) are shown in Figure 3(a). The graphene 2D Raman band (intervalley scattering of two in-plane transverse optical phonons) is directly correlated to the number of layers.[29] The best fit reported in Figure 3(b) is the results of several attempts made using an automated routine. Fitting the band

using a different number of peaks (bigger or lower than four) did not reach convergence and therefore were automat- ically discarded from the software. The starting positions of the peaks were selected by considering the flex points of the original band. Finally, the best fit of the 2D band (≈2670 cm^{-1}) attributed to the graphene embedded into the hybrid matrix (R^2 = 0.9998) has been obtained by a deconvolution with four Lorentzian curves. This result is compatible with the presence of few-layer grapheneflakes in the matrix (Figure 3(b)).[30]

The intensity ratio of the D and G Raman bands, I_D/I_G, is correlated to the number of defects present into graphene. Inten- sity ratios lower than 0.5 indicate low amount of defects.[31] In the case of the graphene flakes embedded into the NIF (Not ImprintedFilms) samples (red curve), this is equal to 0.22, and it signifies that

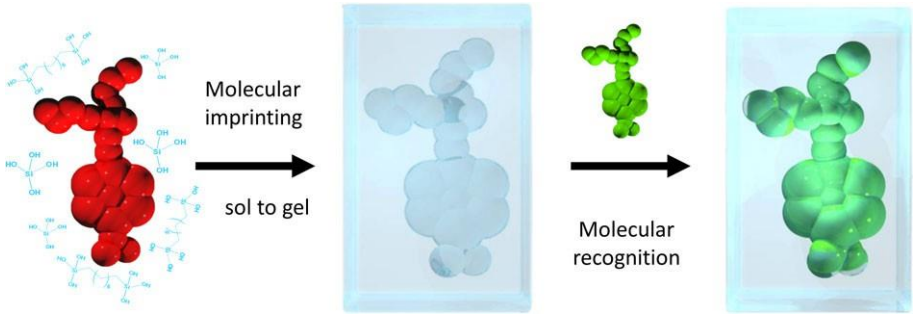

Figure 2. Schematic of the molecular imprinting approach. The siloxane monomers produce a sol that self-assembles around the template molecule (red molecule). The sol to gel transition induces the formation of a molecularly imprinted gel that condenses into a hybrid silica network. The removal of the template molecule leaves molecularly imprinted cavities capable of rebinding selectively structural analogues (green molecule) of the molecular template.

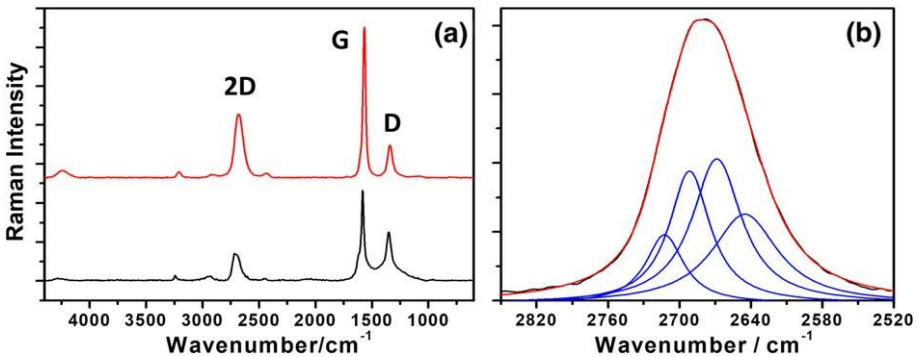

Figure 3. (a) Raman spectra of exfoliated graphene in *N*-Vinyl-2-pyrrolidone (black curve) and exfoliated graphene embedded into the not-imprinted hybrid film (red curve) measured using a 532 nm laser; (b) Lorentzian deconvolution of 2D Raman band of graphene embedded into the hybrid matrix.

the incorporation of graphene into the hybrid film did not intro- duce a significant amount of defects into the graphene structure.

The choice of the template for the MI is crucial because this molecule can be either the same as the target or a

very close structural analogue. In the present work, the direct use of the commercial pesticide paraoxon as a molecular template has two main drawbacks. The first is that paraoxon is really toxic, and therefore, it must be handled very carefully and in the lowest possible amounts. The second issue is that, although very slowly, paraoxon can be hydrolysed in protic solvents,[8] and therefore, the amount used to imprint the cavities would be lower than the estimated theoretical value. For these reasons, it was decided to use, instead, a structural analogue, the diethyl(4-nitrobenzyl)phos-phonate (4NBP), which cannot be hydrolysed (Figure 1).

This molecule differs from the paraoxon only by one oxygen atom that is replaced by a carbon, transforming the hydrolysable 4-nitro-phenyl-phosphate into a not hydrolysable 4-nitrobenzyl- phosphonate, where the phosphorous is directly bound to the carbon (Figure 1). To rule out the intrinsic effect of the matrix, the molecularly imprinted film (MIF) has been always compared with a corresponding not-imprinted film (NIF), embedding graphene but lacking of molecular cavities. Cetyltrimethylammonium bromide (CTAB) has been selected as a micellar template to induce porosity into the hybrid matrix and increase the diffusion rate of the target analyte inside the matrix. The presence of a porous network is expected facilitating the molecular recognition from the cavities and the detection from the graphene flakes. In fact, it has been previously shown that even a small increase in the overall porosity can increase significantly the ERS signal of the analyte.[28]

Molecular imprinting and template removal

The incorporation of the molecular template has been assessed by the Fourier transform infrared (FTIR) absorption spectra of Figure 4. The signals of 4NBP are compared with those of the molecularly imprinted hybrid film thermally treated at 150 °C. The bands, peaking at 1524 and 1348 cm^{-1}, are assigned, respectively, to the asymmetric and symmetric stretching of the 4-nitro-aromatic group. These bands can be unambiguously correlated to the presence of the molecular template, and in fact, they are only detected in the MIF film before washing. On the other hand, the FTIR spectra show that, after washing the film by ultrasonicating them in ethanol, the 4NBP can be completely removed from thehybrid composite films.

The transmission electron microscope (TEM) images (Figure 5) show that both samples are characterised by a homogeneous worm-like interconnected micro-porosity, mostly not organised, with a pore size smaller than 1 nm. Interestingly, the MI procedure does not affect the pores morphology, because not clear differ- ences can be highlighted between the two samples (see also en- larged TEM in Figure S1). The similarity between the MIF and NIF structures and properties is also confirmed by the same hydrophi-licity, 44° of contact angle (see Figure S2).

The thickness of the MIF and NIF hybrid composites has been evaluated through spectroscopic ellipsometry on films deposited onto silicon wafers. To obtain a reliable evaluation before and after the ethanol washing, it was necessary to use a specific Cauchy model capable of fitting the optical properties of the hybrid matrix. The model has been developed by fitting the ellipsometric data of a

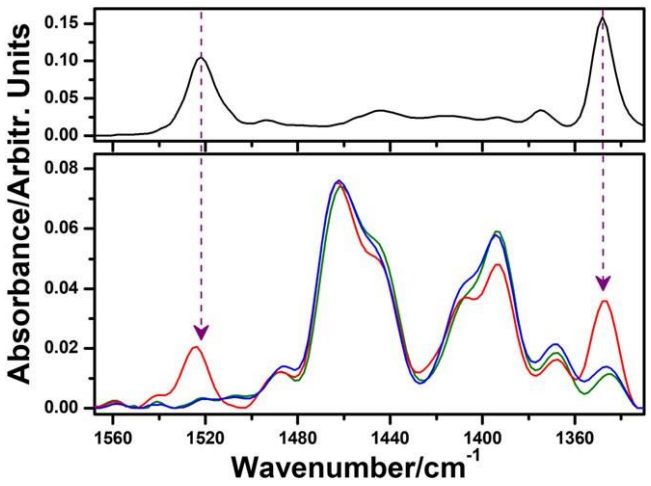

Figure 4. Fourier transform infrared spectra of molecularly imprinted film, before (red curve) and after (blue curve) washing the samples, with respect to not-imprinted film spectrum (green curve). The Fourier transform infrared spectrum of the molecular template (diethyl(4-nitrobenzyl)phosphonate) is reported as a reference (top curve).

dense hybrid film embedding graphene with a standard Cauchy model. The resulting Cauchy parameters have been used to fit properly the porous hybrid MIF and NIF using a Bruggemann effective medium approximation to determine both thickness and porosity. The ellipsometric measurements show a substantial coherence between the thicknesses of the MIF and NIF before and after ultrasonication in ethanol, used to remove both the molecular template and CTAB. In fact, the thickness for MIF and NIF were, respectively, 1133 ± 22 and 1178 ± 14 nm before washing and 1006 ± 30 and 1011 ± 29 nm after washing. In all the cases, thefitting was excellent with a mean square error always lower than 0.16. The overall porosity appeared to be substantially unaffected by the presence of the molecular cavities because, for both MIF and NIF, this increase of about 2% after the sonication in ethanol.

The successful embedding of the molecular template has been also verified by ultraviolet–visible (UV–Vis) spectroscopy on MIF and NIF films deposited onto silica slides before ultrasonication in ethanol (Figure S3(a)). The MIF sample shows a strong absorption peak centred at 273 nm and due to the 4-nitro-benzyl moiety of the molecular template whilst the NIF sample appears to be completely transparent. After washing, the absorption due to the molecular template is no longer detected.

Ultrasonication in ethanol offers another important advantage, which is the possibility of quantifying the number of molecular cavities present in each MIF sample. This parameter allows evaluating the true efficiency of the MI strategy. The amount of molecular cavities in a MIF sample can be determined by UV–Vis spectroscopy. The samples have been fully immersed into a known volume of ethanol (3 ml) and sonicated for 30 min. This procedure has been repeated until the complete disappearance of the molecular template. As shown in Figure S3(b), two washing cycles have been, in general, sufficient to completely remove the template from the MIF. The solutions have been analysed by UV–Vis, and the concentration of 4NBP, removed from the film by the ethanol solution, has been estimated using a calibration curve obtained through a cross-dilution process (Figure S4). The third washing solution did not show any

substantial absorption. The concentra- tion of 4NBP has been determined on the overall volume of ethanol used to ultrasonicate the MIF (9 ml in this case). This corresponds to an upper limit of the 'concentration' of molecularly imprinted cavities present into the MIF volume because not all the imprinted cavities can be actually considered fully active. The density of the molecular cavities in the samples has been calculated by dividing the overall number of 4NBP molecules, washed out from a hybrid matrix, by the corresponding MIF volume (film area × film thick- ness). By taking into account the overall number of micromole of 4NBP in the washing solution, we have therefore estimated the up- per density of molecular cavities into a MIF sample as$4.50 * 10^{-10}$ µmol $µm^{-3}$.

Molecularly Imprinted - Graphene-mediated Enhancement of Raman Scattering for paraoxon

A Raman-based sensing technique making use of a solid-state platform requires a homogeneous distribution and a univocal fingerprint of the analyte. To have a homogeneous deposition of paraoxon onto the surface of the hybrid platform, a small amount of surfactant (CTAB) has been added to the paraoxon solution. CTAB lowers the surface tension of the solution allowing the deposition of a thin liquid layer onto the surface of the sensing platform. Figure 6(a) shows the Raman spectra of the CTAB– paraxon solution deposited onto MIF and NIF substrates. Paraoxon can be clearly identified by two bands peaking, respectively, at 1349 and 1594 cm^{-1}, which have been used to monitor the

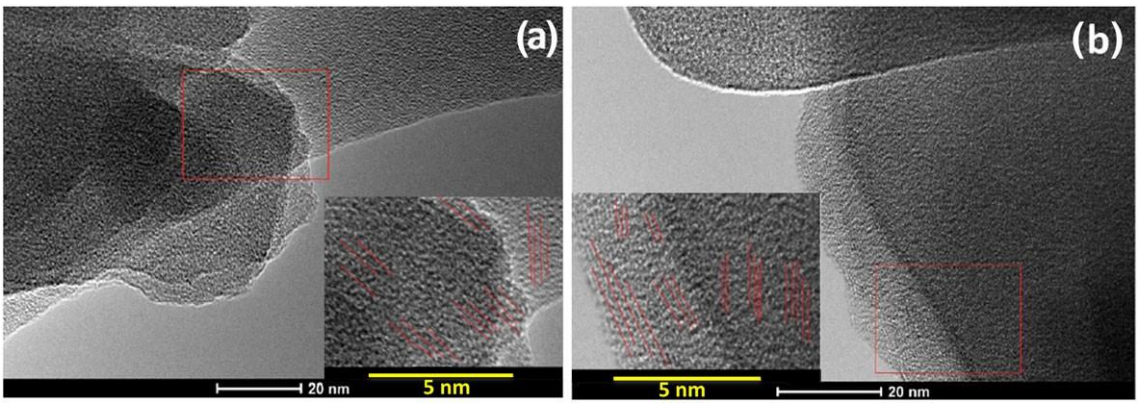

Figure 5. Transmission electron microscope images of not-imprinted film (a) and molecularly imprinted film (b) samples after ultrasonication in ethanol. The enlargements, displaying the partial organisation of the porous structure, are shown as inset.

enhancement of the Raman signal due to the hybrid matrix con- taining only graphene (NIF) with respect to the enhancement due to the matrix containing both graphene and molecular cavities (MIF). To appreciate the

enhancement provided by the different sensing platforms, a bar plot comparing the intensities of paraoxon bands on MIF and NIF substrates is shown in Figure 6(b). The MIF substrate shows a ≈ fourfold increase of Raman enhancement with respect to the NIF; this increase is due only to the presence of mo- lecularly imprinted cavities in GERS platforms. In addition, each re- ported value of the Raman signal is the average of at least five measurements.

Enhancement efficiency per cavity

The efficiency of a sensing substrate in enhancing the Raman scattering signal of an analyte is assessed by using their enhance- ment factor (EF). However, to calculate the EF, the exact number of molecules adsorbed onto the ERS-active surfaces that gives Raman enhancement is required.[32] In fact, the EF is provided by the intensities ratio of the ERS active and not active substrates, corrected by the corresponding number of molecules. This parameter is very important to characterise ERS-active surfaces of plasmonic Ag or Au nanoparticles, but it becomes less significant for 2D ERS-active materials such as graphene. In fact, the ERS activity of these materials is mainly based on a chemical mechanism (CM), whose maximum enhancement is theoretically lower than 10^2, whilst the ERS of the plasmonic nanoparticles can reach up to 10^{12} being based on both CM (max 10^2) and electro- magnetic mechanism (EM) (max 10^9).[24] In both mechanisms, the signal enhancement is distance-dependent, but in the case of the CM, the chemical interaction between the substrate and the analyte is even more important. Previous studies have already shown that the incorporation of exfoliated graphene into porous inorganic or hybrid matrices is capable of giving relatively high AEF (analytical enhancement factor) for Rhodamine 6G, up to 18, when compared with other GERS-active materials.[33]

The present paper focuses on the selectivity ensured by the molecularly imprinted cavities rather than measuring the AEF of the ERS-active versus the not ERS-active substrates. For this reason,

the enhancement efficiency has been calculated considering the increase of only ERS-active substrates, MIF versus NIF. In such a way, it is possible to evaluate the effective impact of the molecular cavities onto the enhancement (MIF), unbiased by the GERS effect because of the graphene embedded into the porous hybrid platform (NIF). We need, therefore, to subtract the signal intensity because of the porous GERS matrix (NIF), I_{NIF}, from that of the molecularly imprinted GERS, I_{MIF}.

$$I_{cavities} = I_{MIF} - I_{NIF} \quad (1)$$

Dividing the $I_{cavities}$ value by the number of cavities illuminated by the laser, it is then possible to determine the enhancement because of the single cavity. Because the Raman signal derives only from the molecules excited within the laser spot area, which for our experimental setup is equal to 0.4 μm^2, it is possible to calculate the effective volume illuminated by the laser considering the thickness of our porous material, ≈1 μm. The resulting laser spot volume (LSV) is equal to 0.4 μm^3 and therefore, considering that we have estimated the upper density of the molecular cavities into the MI-GERS as $4.50 * 10^{-10}$ μmol μm^{-3}, we can calculate the upper value of analyte molecules using the corresponding values of molecular cavities that can be filled in. In conclusion, from the LSV of our experimental setup and the density of the cavities into the MI-GERS, we can assume that the upper number of molecules, $N_{cavities}$, adsorbed into the porous MI-GERS, illuminated by the laser and accountable for the '*molecular*' enhancement, is $1.84 * 10^{-10}$ μmol. It is now possible to estimate the enhancement efficiency (EE) per micromole of cavities, EE_{cavity} (at 1349 cm^{-1}) as it follows:

$$EE_{cavity} = I_{cavities} / N_{cavities} \quad (2)$$

In our case, this value is equal to 1.47 * 10^{12} count * μmol^{-1}, but it is also important to underline that this value is dependent on laser power, excitation wavelength and Raman mode, and it is an underestimation because of the overestimated value of the LSV. This means that a very small number of molecular cavities can provide a quite remarkable amplification of selective Raman enhancement. However, it is important to underline that there is

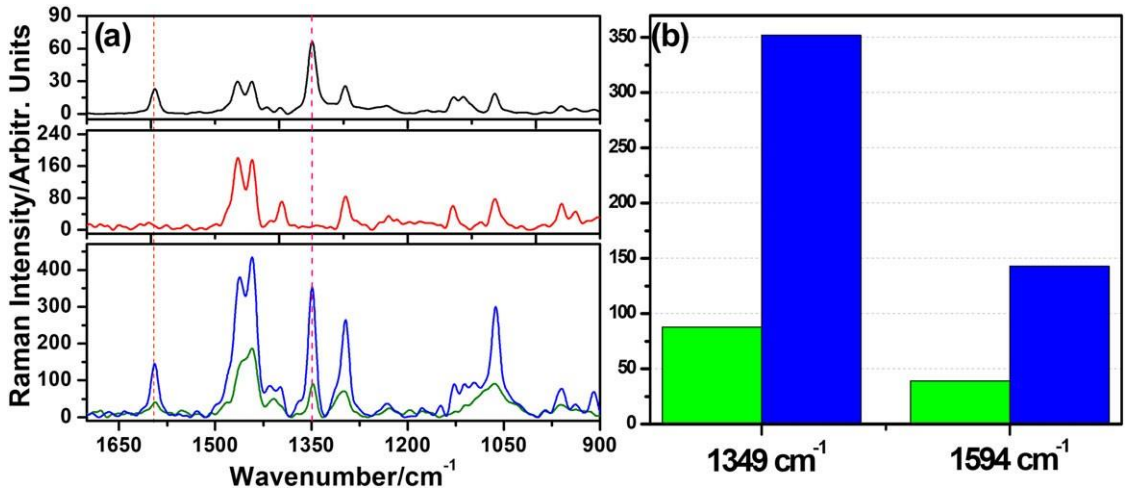

Figure 6. (a) Raman spectra of paraoxon solution containing cetyltrimethylammonium bromide (CTAB) deposited onto not-imprinted film (green curve) and molecularly imprinted film (blue curve) substrates. The spectra of paraoxon solution containing CTAB deposited onto silica substrate (black curve) and pure CTAB solution deposited onto MIF substrate (red curve) are reported as references. (b) Bar plot comparing the band intensities of a paraoxon solution deposited onto not-imprinted film (green) and molecularly imprinted film (blue) at 1349 and 1594 cm^{-1} Raman mode.

a limit for increasing the density of cavities into a porous film because an increasing concentration of molecular template could lead to undesired molecular aggregations that produce unselective cavities. The EE_{cavity}, however, is not directly comparable with the AEF commonly used. In this kind of molecularly imprinted matrices, in fact, it is not possible to estimate a reliable AEF because, the overall porosity of both molecularly imprinted and not imprinted films is almost the same (i.e. the contribution of the molecular cavities to the overall porosity is negligible). The EE per micromole of cavities is instead intended to emphasise the enhancement provided solely by the presence of molecular cavities. The origin of this improvement is still not completely clear, however, we hypothesise that the molecular cavities operate a selective preconcentration of a specific analyte in close proximity of graphene layers. This would make easier the interaction between the analyte and graphene, thus promoting the Graphene-mediated enhancement of Raman scattering.

Measurements reproducibility of Molecularly Imprinted - Graphene-mediated

Enhancement of Raman Scattering substrates

Two important properties of the material employed for sensing purposes are the mechanical and hydrolytic stabilities in the measuring environment. In addition, the durability is a requirement to recycle the platform more than once.

Figure S5 shows the intensity of the 1349 cm^{-1} Raman band of paraoxon in NIF and MIF samples after each washing step. The measured intensities show only a very small change that can be quantified in 4% for NIF and 1% for MIF. The statistical variability in the MIF samples is lower because of the higher signal to noise ratio. The high reproducibility of the measures is evidencing that the washing procedure removes all the paraoxon residues from the matrix without producing any degradation. Both MIF and NIF hybrid substrates can be recycled at least 5 times without any loss of performance. The sensitivity of the MI-GERS platform has been verified by measuring constant volumes of paraoxon in ethanol and CTAB with decreasing concentrations (from 10^{-3} to 10^{-7} M) (Figure 7(a)). At first, ethanol has been chosen as a solvent because the solubility of paraoxon is higher than in water. The results show that MI-GERS is able to detect paraoxon in concentrations as low as 10^{-5} M. At lower concentrations, the signal to noise ratio (see experimental for detailed calculation) is too low to allow a reliable measurement. Figure S6(a) shows that there is a good correlation between signal intensity and concentration of paraoxon in ethanol. Because the presence of organophosphate in the ground water has a huge environmental impact, it is of paramount importance to establish a protocol that allows evaluating the paraoxon concentra- tion in water. Given the impossibility of obtaining a homogeneous deposition of a water solution of paraoxon directly onto a MI-GERS surface, even after adding CTAB, it was decided to operate a controlled dilution of the pesticide solution. Different paraoxon aqueous solutions, with a concentration ranging from 10^{-3} to 10^{-5} M, have been prepared and then diluted 1:10 with ethanol. The corresponding intensity of the Raman signals was lower than in ethanol because the analysis was effectively performed onto a diluted solution (Figure 7(b)). The paraoxon concentra- tion in the water-ethanol mixtures is, in fact, one-tenth of the original concentrations in water and this increases the limit of detection affecting therefore the sensitivity. Likewise the etha- nol samples, the intensity of the Raman signal of the water solu-tion offers a good linear correlation with the paraoxon concentration (Figure S6(b)).

Selectivity of Molecularly Imprinted - Graphene-mediated Enhancement of Raman Scattering substrates

One of the main issues related to the determination of specific pollutants is the selectivity of the analytical technique in recognising and detecting specific compounds. The interference of similar molecules could affect the measurement. To overcome this problem, the pairing of two different techniques, i.e. a separa- tion followed by a specific detection, is the most used approach.

However, these 'hyphenated' techniques are cumbersome bench-lab facilities, time-consuming, not very cheap and with some environmental impact (i.e. large use of solvents or gases in chromatography techniques). The hybrid organic–inorganic platform developed in this work has, instead, proved to be a quick, cost-effective and environmental-friendly method to determine paraoxon in ethanol and in water/ethanol mixtures. The most important feature is the degree of molecular selectivity that MI-GERS is able to reach. This property has been verified by com- paring the

capability of a MIF sample versus a NIF in detecting

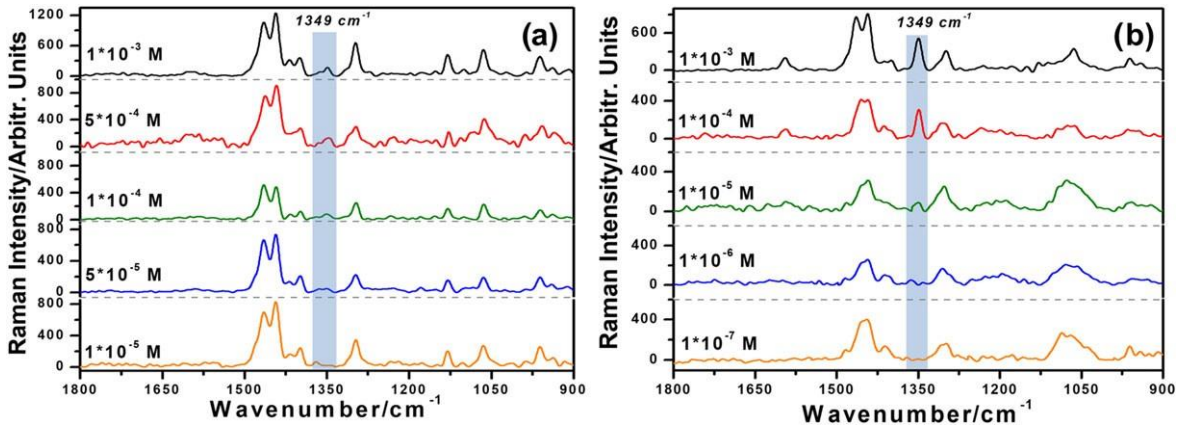

Figure 7. (a) Raman spectra of different paraoxon solutions (ranging from 10^{-3} to 10^{-7} M) deposited onto molecularly imprinted film and containing cetyltrimethylammonium bromide; (b) Raman spectra of different paraoxon solutions (ranging from 10^{-3} to 10^{-5} M) deposited onto molecularly imprinted film, containing cetyltrimethylammonium bromide and diluted 1/10 with ethanol.

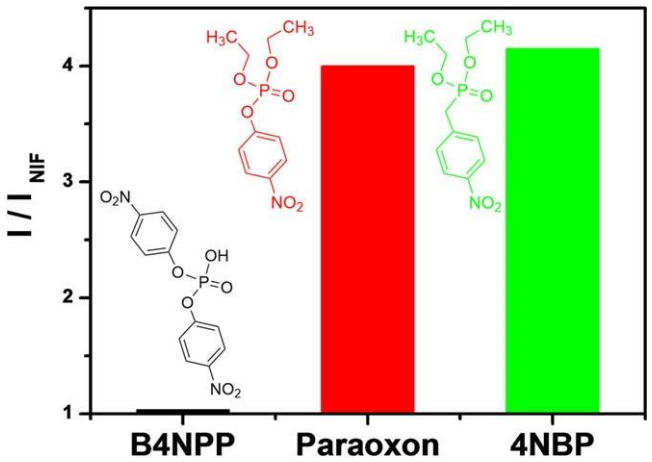

Figure 8. Bar plot showing the selectivity of molecularly imprinted film material towards solutions of bis(4-nitrophenyl) phosphate, diethyl(4- nitrobenzyl)phosphonate and paraoxon (for 1349 cm^{-1} Raman mode) with respect to not-imprinted film (normalised to 1).

the same amount of 4NBP, paraoxon, and, finally, a structural analogue, bis(4-nitrophenyl) phosphate (B4NPP).

Figure 8 shows a bar plot with the intensity of the 1349 cm^{-1} Raman band of the three different organophosphates

measured on MIF samples normalised by their corresponding intensities on the NIF (I_{MIF}/ I_{NIF}). The highest signal enhancement, 4.15-fold increase, is obtained, as expected, with the 4NBP, which is the molecular template used to imprint the molecular cavities. The selectivity towards paraoxon is very similar to the molecular template exhibiting a fourfold increase. It is important to underline that the structures of these two molecules differ only by an oxygen atom. On the contrary, the third molecule, B4NPP, is an organophosphate characterised by the presence of two 4-nitro- aromatic groups (Figure 1). The structure is consequently more bulky and difficult to fit inside the molecularly imprinted cavity. The result of this structural difference is essentially a lack of signal enhancement because the imprinted sample shows a negligible signal increase (equal to 1.04). This response can be justified only assuming that, in the latter case, the MIF could not operate a molecular recognition of the analyte and the subsequent signal enhancement. In other words, the MI-GERS are characterised by two degrees of selectivity, one controlled by the presence of a specific Raman fingerprint signal associated with a functional group of the analyte, and the second, more specific, controlled by the presence of the imprinted cavities. This allows the molecular exclusion of compounds that do not fit into the cavities. The combined effect of these two degrees of selectivity provides a unique amplification of a specific analyte that cannot be achieved by using GERS and MI separately.

Conclusions

Chemical design of a porous hybrid organic–inorganic film has granted the successful fabrication of a sensing platform characterised by molecular cavities and graphene. This GERS- active material combines a number of different features, such as accessible microporosity, mechanical and chemical stabilities. The system, used as a sensing platform for Raman detection of organophosphates, shows a high selectivity provided by the molecular cavities. In particular, the high sensing efficiency is due to the combination of the graphene-mediated Raman enhancement and an additional enhancement achieved through molecular recognition. We have proved that, by using a MI-GERS approach, a very small number of molecularly imprinted cavities is capable of recognising selectively paraoxon, returning a significant signal enhancement per micromole of cavities equal to $1.47 * 10^{12}$ count * μmol^{-1}. The general strategy of shaping the porosity for achieving selective GERS sensing has hence proved to be a cost effective and environmental friendly alternative to the actual 'hyphenated techniques' commonly used for detecting pollutants in water. Moreover, this combined approach has proved to be very promising for the future development of integrated portable devices for environmental monitoring.

Experimental section

Chemicals and materials

N-Vinyl-2-pyrrolidone (Sigma-Aldrich), graphite (Sigma-Aldrich), tetraethoxysilane (Aldrich, >99% purity), 1,8-bis(triethoxysilyl)oc- tane (Aldrich, 97% purity), CTAB (Sigma-Aldrich, 99%), ethanol (Fluka, >99.8%), *iso*-propyl-alcohol (Fluka, >99.8%), hydrochloric acid (Sigma-Aldrich, 37% wt/wt), water (milli-Q), 4NBP

(Sigma-Aldrich, 98%), diethyl 4-nitrophenyl phosphate (paraoxon®) (Fluka, 97.6%) and B4NPP (Sigma-Aldrich, 99%) were used as received without further purification. Silica slides and silicon wafers were employed as substrates for film deposition. Before use, the silica slides and silicon wafers were washed with water, acetone and ethanol then dried with compressed air and thermally treated at 600 °C in oven for 1 h. The substrates were then pretreated with a solution (H_2O: H_2O_2: $NH_3{\cdot}H_2O$ = 5: 1: 1)before film deposition.

Synthesis of molecularly imprinted film and not-imprinted film platforms

Eight millilitre of ethanol, 1 ml of tetraethoxysilane, 2.126 ml of 1,8-bis(triethoxysilyl)octane , 0.3 ml of water and 0.05 ml of 1 M hydrochloric acid were added in a glass vial (molar ratios, tetraethoxysilane: 1,8-bis(triethoxysilyl)octane : ethanol: water: hydrogen chloride = 1: 1: 30: 6.4: 0.025) under stirring to prepare a hybrid sol. After 10 min, 0.02 g CTAB dissolved in 0.5 ml ethanol (molar ratio, tetraethoxysilane: CTAB = 1: 0.012; [Si]: CTAB = 1: 0.004) were added to the hybrid sol that was then left to react under stirring for 2 h at room temperature in a closed vial. One hundred fifty microlitre of the EG-NVP dispersion (see Supporting Information: Preparation of NVP dispersion of exfoliated graphene) were then added to the 5 ml of the hybrid sol and kept under stirring. After 30 min, 60 µl of 4NBP (1 M) were dispersed into the hybrid sol containing EG-NVP and left to react under stir- ring for 2 h before depositing molecularly imprinted porous films (MIF) by spin coating. The films were deposited on silicon and sil- ica substrates with a spinning rate of 1000 rpm for 40 s and then 500 rpm for 20 s. At first, the films were kept 12 h into oven at 60 °C and then treated at 150 °C for 1 h. NIFs were prepared by exactly the same procedure, only without adding the template molecule (4NBP) in the sol. The appropriate amount of ethanol (60 µl) was added into the sols to have the same total volumein both the solutions.

Removal of the molecular template diethyl(4-nitrobenzyl)phosphonate

Removal of the molecular template diethyl(4-nitrobenzyl)phosphonate Molecularly imprinted films were washed with 3 ml of ethanol and ultrasonicated for 30 min (99% power, 400 VA). After each washing step, the resulting ethanol solution was analysed by UV–Vis spectroscopy. The amount of B4NBP removed from the film was estimated by using the extinction coefficient at 270 nm, ε270,equalto 10 579 $M^{-1}cm^{-1}$, obtained from a cross-dilution calibration curve (Figure S4). The MIF-EG was washed 3 times, and the overall concentration of B4NBP removed from each film was determined as the sum of the three washing steps (overall 4NBP contained into 9 ml of ethanol). In order to make sure that all samples underwent the same treatment, NIF-EG sample was also washed in the same way as MIF-EG.

Characterisation

Fourier transform infrared spectra were recorded in transmission mode between 4000 and 400 cm^{-1} by averaging 256 scans with 4 cm^{-1} of resolution using an interferometer Bruker infrared Vertex 70v. Optical absorption of the hybrid films was measured by a Nicolet Evolution 300 UV–Vis spectrophotometer in the range of 200–800 nm with a bandwidth of 1.5 nm. TEM images were obtained by using a FEI TECNAI 200 microscope working with a field emission electron gun

operating at 200 kV. Raman analysis was performed by using a Bruker Senterra confocal Raman microscope with a laser excitation wavelength of 532 nm, 5 mW of nominal power and a 100× objective. The spectra were recorded in the 70–4500 cm^{-1} range, with a resolution of 9 cm^{-1}, an integration time of 3 s and six co-additions. The laser spot diameter was calculated by using the following formula 1.22 * λ/NA (first Airy disk), where λ is the laser wavelength (in nm), and NA is the numerical aperture of the microscope objective. In our case, we have used an infrared laser (λ=532 nm), and an objective whose NA is 0.90. The corresponding laser spot diameter is 721 nm. The detection limit has been assessed by using the signal-to-noise ratio of the band centred at 1349 cm^{-1} (SNR_{1349}). The SNR_{1349} has been calculated as the ratio between the average peak height above the baseline (*S*) and the standard deviation of the peak height (σ_{1349}).[34] S has been obtained by averaging the band intensity at 1349 cm^{-1} of five different measurements, whilst σ_{1349} has been obtained by subtracting two different Raman spectra collected from the same sample region and calculating the standard deviation in the 1450–1140 cm^{-1} range. The spectra with a SNR_{1349} lower than five have been considered under the detection limits and discarded. A Woollam-α spectroscopic ellipsometer with fixed angle geometry was used for measuring the thickness of the films deposited on silica substrates. The thickness was estimated by fitting the experimental data with a model developed using dense hybrid films deposited onto silica substrates. The fit showed an average mean square error always lower than 0.16. The hydrophobicity of the hybrid films was evaluated using a Dataphysics OCA 20 by measuring the contact angle of 5 µl water droplets deposited onto the hybrid films coated on silica substrates. The contact angle was obtained by averaging atleast five measurements.

Evaluation of graphene-mediated enhancement of Raman scattering and molecular selectivity in ethanol

The ERS was measured on MIF and NIF films. Raman measure- ments were obtained by using a Bruker Senterra confocal Raman microscope using a laser excitation wavelength of 532 nm, 5 mW of nominal power and a 100× objective. The spectra were recorded

disposing off the samples with organophosphate compounds. UV–Vis analysis was performed on the washing solutions after each cleaning cycle to verify the absence of residues from previous measurements. B4NPP and 4NBP, used as molecular probes, were

determined by following exactly the same procedure as for paraoxon. The reusability of MIF was evaluated by casting 20 µl of 10^{-3} M paraoxon solution onto the film. After each Raman measurement, the samples were washed by ultrasonication in ethanol to ensure the complete removal of paraoxon traces.

Evaluation of graphene-mediated enhancement of Raman scattering in water

Different concentrations of paraoxon aqueous solution ($1{\cdot}10^{-3}$, $5{\cdot}10^{-4}$, $1{\cdot}10^{-4}$, $5{\cdot}10^{-5}$, $1{\cdot}10^{-5}$ M) were prepared by diluting paraoxon-acetonitrile solution with water. Before detection, 200 µl of paraoxon® aqueous solution were diluted into 1.8 ml of ethanol. After stirring for 2 h, 20 µl of solution was deposited onto the MIF film and dried at room temperature. The film waswashed with ultrasonication in ethanol before and after each measurement.

Acknowledgements

A. Mariani and V. Alzari are kindly acknowledged for the preparation of the graphene dispersion in NVP. Regione Autonoma Sardegna is acknowledged for funding this project through CRP 30 L.R. 7/2007 ‘Bando Capitale Umano ad Alta

Qualificazione annualità 2015'. This work was partially supported by the project 'Mi ADATTI E L'ABBATTI'- INSTM-Regione Lombardia project INSTMRL6. Italian Ministry of Foreign Affairs and International Cooperation (MAECI) is acknowledged for funding this work through the cooperationproject "GRAPEMAT" (PGR04266) between Italy and China.

References

[1] X. Yu, W. Zhang, P. Zhang, Z. Su, *Biosens. Bioelectron.* 2017, *89*, 72.
[2] H. Wei, S. M. Hossein Abtahi, P. J. Vikesland, *Environ. Sci. Nano* 2015, *2*, 120.
[3] S. Lazar, I. Egoz, R. Brandeis, S. Chapman, E. Bloch-Shilderman, E. Grauer, *Toxicol. Appl. Pharmacol.* 2016, *310*, 87.
[4] L. Kapka-Skrzypczak, M. Cyranka, M. Skrzypczak, M. Kruszewski, *Ann. Agric. Environ. Med.* 2011, *18*, 294.
[5] D. Guodong, W. Pei, T. Ying, Z. Jun, G. Yu, W. Xiaojin, S. Rong, W. Guoquan, S. Xiaoming, *Environ. Sci. Technol.* 2012, *46*, 2911.
[6] C. Hyland, O. Laribi, *Environ. Res.* 2017, *156*, 559.
[7] G. Aragay, F. Pino, A. Merkoçi, *Chem. Rev.* 2012, *112*, 5317.
[8] D. Carboni, L. Malfatti, A. Pinna, B. Lasio, Y. Tokudome, M. Takahashi, P. Innocenzi, *New J. Chem.* 2013, *37*, 2995.
[9] D. Carboni, B. Lasio, L. Malfatti, P. Innocenzi, *J. Sol-Gel Sci. Technol.* 2016, *79*, 395.
[10] D. Marongiu, D. Carboni, L. Malfatti, P. Innocenzi, *J. Mater. Chem.* 2012, *22*, 20498.
[11] G. Marrazza, *Biosensors* 2014, *4*, 301.
[12] P. Kumar, K.-H. Kim, A. Deep, *Biosens. Bioelectron.* 2015, *70*, 469.
[13] Š. Štěpánková, K. Vorčáková, *J. Enzyme Inhib. Med. Chem.* 2016, *31*, 180.
[14] W. Zhang, X. Ge, Y. Tang, D. Du, D. Liu, Y. Lin, *Analyst* 2013, *138*, 5431.
[15] N. Chauhan, C. S. Pundir, *Electrochim. Acta* 2012, *67*, 79.
[16] S. Zhang, Z. Jiao, W. Yao, *J. Chromatogr. A* 2014, *1371*, 74.
[17] A. M. Shrivastav, S. P. Usha, B. D. Gupta, *Biosens. Bioelectron.* 2016, *79*,150.
[18] X. Yan, H. Li, Y. Yan, X. Su, *Food Chem.* 2015, *173*, 179.
[19] X. Wu, Y. Song, X. Yan, C. Zhu, Y. Ma, D. Du, Y. Lin, *Biosens. Bioelectron.* 2017, *94*, 292.
[20] L. Chen, X. Wang, W. Lu, X. Wu, J. Li, *Chem. Soc. Rev.* 2016, *45*, 2137.
[21] S. Pang, T. Yang, L. He, *Trends Anal. Chem.* 2016, *85*, 73.
[22] X. Ling, S. Huang, S. Deng, N. Mao, J. Kong, M. S. Dresselhaus, J. Zhang, *Acc. Chem. Res.* 2015, *48*, 1862.
[23] I. Alessandri, J. R. Lombardi, *Chem. Rev.* 2016, *116*, 14921.
[24] X. Ling, L. Xie, Y. Fang, H. Xu, H. Zhang, J. Kong, M. S. Dresselhaus, J. Zhang, Z. Liu, *Nano Lett.* 2010, *10*, 553.
[25] D. Carboni, B. Lasio, V. Alzari, A. Mariani, D. Loche, M. F. Casula, L. Malfatti, P. Innocenzi, *Phys. Chem. Chem. Phys.* 2014, *16*, 25809.
[26] P. Innocenzi, L. Malfatti, D. Carboni, *Nanoscale* 2015, *7*, 12759.
[27] D. Carboni, A. Pinna, L. Malfatti, P. Innocenzi, *New J. Chem.* 2014, *38*, 1635.
[28] D. Carboni, Y. Jiang, M. Faustini, L. Malfatti, P. Innocenzi, *ACS Appl. Mater. Interfaces* 2016, *8*, 34098.
[29] A. C. Ferrari, *Solid State Commun.* 2007, *143*, 47.
[30] L. M. Malard, M. A. Pimenta, G. Dresselhaus, M. S. Dresselhaus, *Phys. Rep.* 2009, *473*, 51.
[31] L. G. Cançado, A. Jorio, E. H. M. Ferreira, F. Stavale, C. A. Achete,

R. B. Capaz, M. V. O. Moutinho, A. Lombardo, T. S. Kulmala, A. C. Ferrari, *Nano Lett.* 2011, *11*, 3190.
[32] E. C. Le Ru, E. Blackie, A. M. Meyer, P. G. Etchegoin, *J. Phys. Chem. C* 2007, *111*, 13794.,
[33] D. Carboni, B. Lasio, D. Loche, M. F. Casula, A. Mariani, L. Malfatti, P. Innocenzi, *J. Phys. Chem. Lett.* 2015, *6*, 3149.
[34] R. L. McCreery, *Raman Spectroscopy for Chemical Analysis*, John Wiley & Sons, New York, 2000.